British Journal of Applied Science & Technology
4(17): 2477-2488, 2014

SCIENCEDOMAIN *international*
www.sciencedomain.org

No Frequency Reuse: Wearable Steerable MIMO Microstrip Antenna Array for Mobile Ad Hoc Applications

Taha A. Elwi[1,2,3*], Sa'ad Al-Frieh[1], Mohammed Al-Bawi[1] and Mohammed Noori[1]

[1]Department of Communication, Al-Mammon University Collage, Baghdad, Iraq.
[2]Department of Electronics and Communication, University of Baghdad, Baghdad, Iraq.
[3]Institute of Mathematical Research INSPEM, University Putra Malaysia UPM, Serdang. 43400, Selangor, Malaysia.

Authors' contributions:

This work was carried out in collaboration between all authors. Author Taha designed the antenna design and supervised the numerical simulations. The first draft of the manuscript wrote by the second and the third authors. Author Noori managed literature searches. All authors collaborated to finalize the manuscript. All authors read and approved the final manuscript.

Original Research Article

Received 28th December 2013
Accepted 17th February 2014
Published 28th April 2014

ABSTRACT

Aim: The principle of eliminating the frequency reuse in the mobile Ad Hoc system among the sectors of the unit cell using Multi Inputs Multi Outputs (MIMO) antenna array is investigated in this paper.
Antenna Design: The size of the proposed antenna array is 10×10 cm^2 to obtain a bandwidth around 1 GHz. The single antenna element is constructed from sub-patches that are connected with feeding network through pin diodes, as switches, that are mounted on an FR-4 substrate.
Antenna Performance: The antenna elements are characterized from 0.8 GHz to 2 GHz in terms of *S*-parameters and radiation patterns with different switching OFF/ON categories.
Methodology: A numerical investigation based on Finite Integral Techniques (FIT) of Time Domain (TD) formulations is conducted using CST MWS to evaluate the antenna performance. A Frequency Domain (FD) solver based on CST formulations is conducted for validation.

**Corresponding author: E-mail: taelwi@ualr.edu;*

Results: It is found the antenna shows insignificant coupling around 1.2 GHz and 1.6 GHz. Furthermore, the radiation patters of the antenna are found to be in the end fir direction with phase change of about 120^{o} among antenna sectors. The antenna provides absolute gain of 2 dBi at 1.2 GHz and 2.9 dBi at 1.6 GHz. It is found that the proposed antenna behaves like highly directive end fire antenna at the main lobe direction around 1.6 GHz. Moreover, it is found that the antenna array exhibits insignificant coupling among each other around this frequency.
Conclusion: The performance and structure of the proposed design allows the use with wearable Ad Hoc mobile systems without the need for frequency reuse by steering the radiation patterns of the antenna sectors through switching antenna branches. Finally, an excellent agreement has been achieved between the regarded results from TD and FD solvers.

Keywords: Ad Hoc; Array; Wearable devices; FIT; TD; FD.

1. INTRODUCTION

Decreasing the correlation between conventional antennas mounted on physically miniaturized arrays is one of the most substantial demands in MIMO systems [1]. However, convent antennas face a severe coupling in their arrays at the near-field due to the diffraction from finite-ground planes and exteriors surface waves [2]. Therefore, mutual coupling reduction has become a very demand feature in the design of antenna structure.

On the other hand, antenna array based on different patch configurations were performed for high gain, beam forming, and high diversity applications [3-6], however, the mutual coupling resulted from mutual coupling was addressed as an important issue in most MIMO applications. This is due to the fact of the surface wave propagation among patches elements leading to sever effects on the antennas performance in their arrays [7-8]. Moreover, the mutual coupling depends on the separation distance between the adjacent elements and their feed orientation [9-11].

In the literature, to overcome the negative effects of the mutual coupling, several traditional approaches were introduced in [12-15] such as cavity backing and substrate removal in the miniaturized antenna arrays. In [12], a pure reactance was introduced between antennas at the resonance frequency to realize a separated network from connecting a lossless network between the input ports and the antenna ports. While in [13], transmission lines as antenna decouplers were involved to reduce the mutual coupling effects, however; such kinds of the decouplers are narrowband and restricted with the antenna bandwidth. The mutual coupling between antenna elements was mitigated in [14] through sharing a defected ground plane with resonant slits. A different strategy was presented in [15] by introducing split-ring resonator magnetic inclusions between closely-separated monopole to increase the isolation. Electromagnetic Band Gap (EBG) defects on the ground planes of the microstrip antennas were introduced as nonconventional approaches for mutual coupling reduction as in [16-21]. However, the most manufacturing processes that associated with such approaches are complicated [16]. Nevertheless, the EBG structures in the ground plane increases the back radiation from antenna array that limits their use in wearable devices in close to the human body [22]. In addition to that, the EBG defects on the ground plans blocking the surface waves in a particular frequency band as presented in [16-30]. All these attempts show narrow bandwidth over the frequency of interest such as a fork-like planar EBG in [26] at 5.4 GHz, a mushroom-EBG matrix at 5.8 GHz in [17], a dumbbell-shape structure [29] at 5.6 GHz, and a C-shaped EBG array [30] at 5.5 GHz. Another reported

studies showed mutual coupling reduction at 4.18 GHz [16] and 12.2 GHz with two different EBG defects [31] and [32].

We are investigated in this paper the use of directive sectors based on three patches to act as radiation directors to decrease the mutual coupling effects between the array sectors within a miniaturized profile. The proposed array performance is investigated using CST MWS numerical formulations [33]. The organization of this paper is stated as: In Section II, the proposed antenna array features are discussed. The performance of the antenna array is presented in Section III. Lastly, in Section IV, the accomplishments of the proposed paper are concluded.

2. ANTENNA DESIGN AND METHODOLOGY

The proposed antenna array is based on three main sectors mounted on a circular substrate and fed by coplanar transmission line network with three ports as seen in Fig. 1(a). The individual sector is constructed from three patches fed with a transmission line network as presented in Fig. 1(b). Generally, the microstrip antenna array is shaped circularly; see Fig. 1(c), to achieve high diversity in the radiation patterns of the antenna elements. The patches and the ground planes are considered as PEC layer mounted on a lossy dielectric, ε_r=4.3 and *tan*δ=0.025, FR-4 substrate. The three patches are separated with 120° rotationally around the *z*-axis at the origin. The dimensions and locations of the patches are listed in Table 1 according to Fig. 1(b). The location of the feeding position to the patch is listed in Table 1 from the center of the array. Three sectors are used for full spatial converge, where, each sector covers 120°.

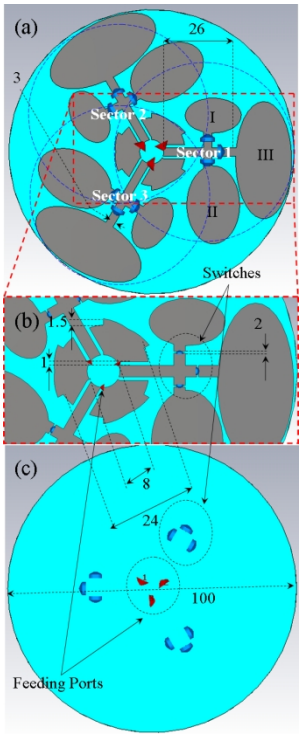

Fig. 1. Antenna dimensions and features in (mm): (a) Front panel, (b) Single antenna sector, and (c) Back panel

Table 1. Patch dimensions, locations, and feeding position in (mm)

Patch	Dimensions (Major × Minor)	Location (x, y)	Feed (X_{offset}, Y_{offset})
I	12 × 6	(22, 13)	(20, 7)
II	18 × 9	(22, -19)	(20, -6)
III	26 × 13	(40, -3)	(30, 0)

3. ANTENNA PERFOMANCE AND DISCUSSION

To study the performance of the proposed antenna array, in terms of S-parameters, gain, and radiation patterns, a full wave simulation based on FIT formulations are invoked using CST MWS [7] as follow:

3.1 Antenna Performance based on Single Sector Element

A numerical study is performed on a single sector element to evaluate the S_{11} and radiation patterns in this section. It is found when all branches are ON; the sector exhibits three resonance modes as seen in the S_{11} as seen in Fig. 2. However, when the second patch is switched OFF only, two modes appear at 1.23 GHz and 1.83 GHz. By switching the first and the second patch OFF, the antenna shows a mode at 1.23 GHz, while the second mode is appeared due to the harmonic generation.

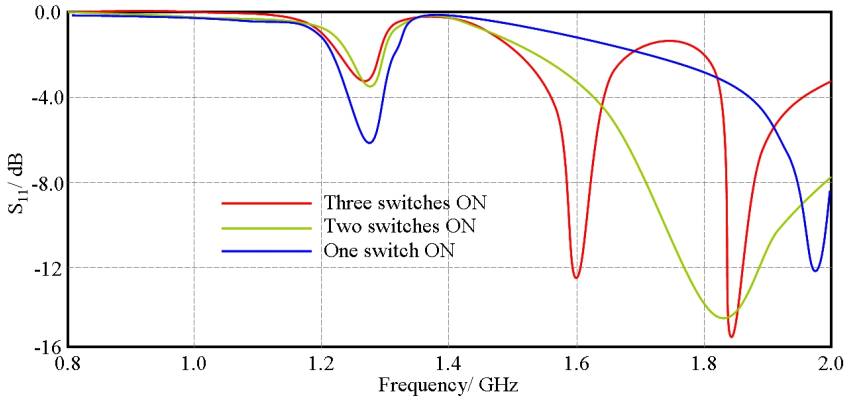

Fig. 2. The S_{11} spectra of the three patches of a single sector.

The radiation patterns of the antenna elements at the three scenarios are presented in Fig. 3 in the *E*- and *H*-planes at 1.2 GHz and 1.6 GHz. The radiation patterns of the antenna array are studied at these frequencies for MIMO applications systems [15].

3.2 Antenna Performance based on Array Structure

In this section, the antenna array performance is investigated by switching the patches of the single sector elements sequentially in their array structure. As seen in Fig. 4, the S-parameters in terms of S_{11}, S_{12}, and S_{13} are displayed by switching the antenna branches. It is found from switching the all patches on, the antenna shows three modes at 1.18 GHz, 1.62 GHz, and 1.82 GHz as seen in Fig. 4(a). However, by switching OFF patch II, two

modes appear at 1.23 GHz and 1.83 GHz. After switching only the third patch ON, the antenna shows a mode at 1.23 GHz and the second mode is appeared due to the second harmonic generation.

In Fig. 4(b), the coupling effects between the sector 1 and sector 2 is presented. When three antenna branches are switched on, the antenna array shows the minimum coupling at 1.18 GHz, while, it shows higher coupling at 1.23 GHz and 1.82 GHz. By switching on the big and small branches on, the antenna provides -10 dB at 1.23 and 1.83 GHz. Now, after switching the big branch on, the antenna presents about -9 dB at 1.23 GHz. The coupling effects between the sector 1 and sector 3 is performed in Fig. 4(c). A higher coupling is found to be when three antenna branches are on at 1.18 GHz, 1.23 GHz, and 1.82 GHz. When the big and small branches are switched on, about the same coupling effect is obtained between sector 1 and sector 2 in Fig. 4(b). The lower coupling effect is achieved by switching only the big branch on at 1.23 GHz.

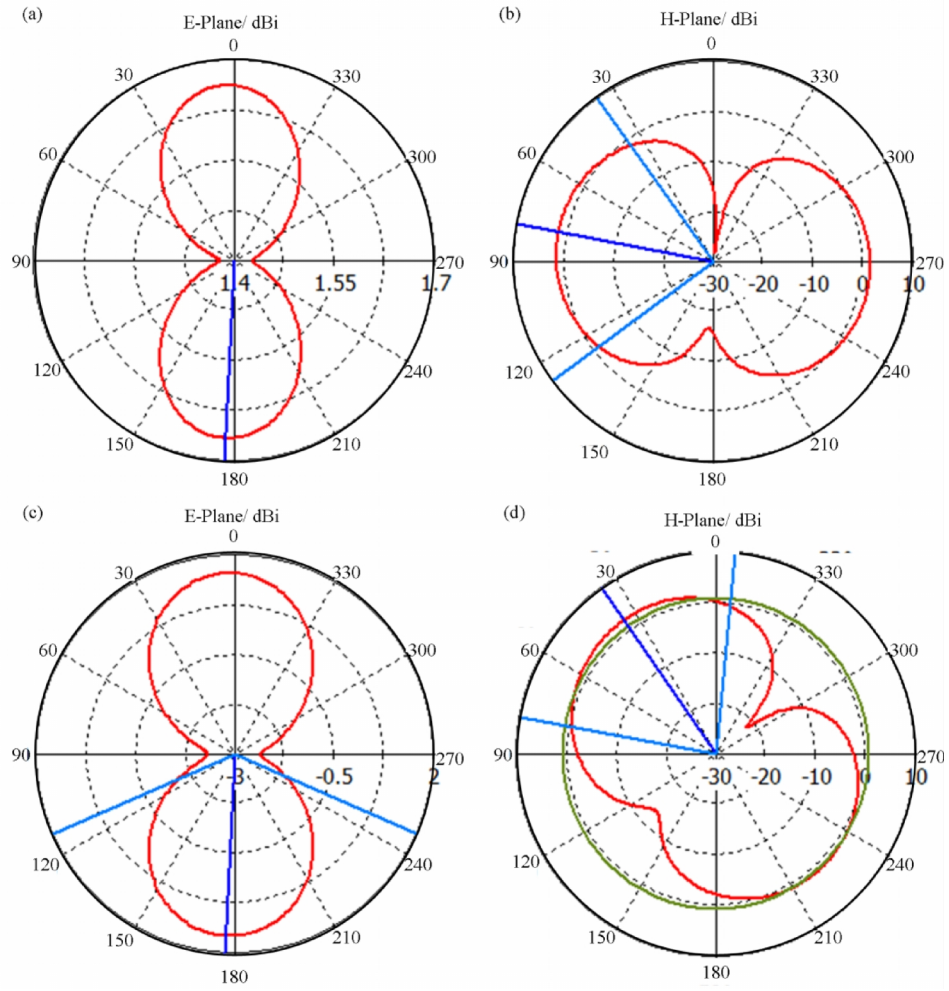

Fig. 3. Far field radiation patterns: (a) E-plane at Theta = 90° and (b) H-plane at Phi = 90° for 1.2 GHz. (c) E-plane at Theta = 90° and (d) H-plane at Phi = 90° for 1.6 GHz.

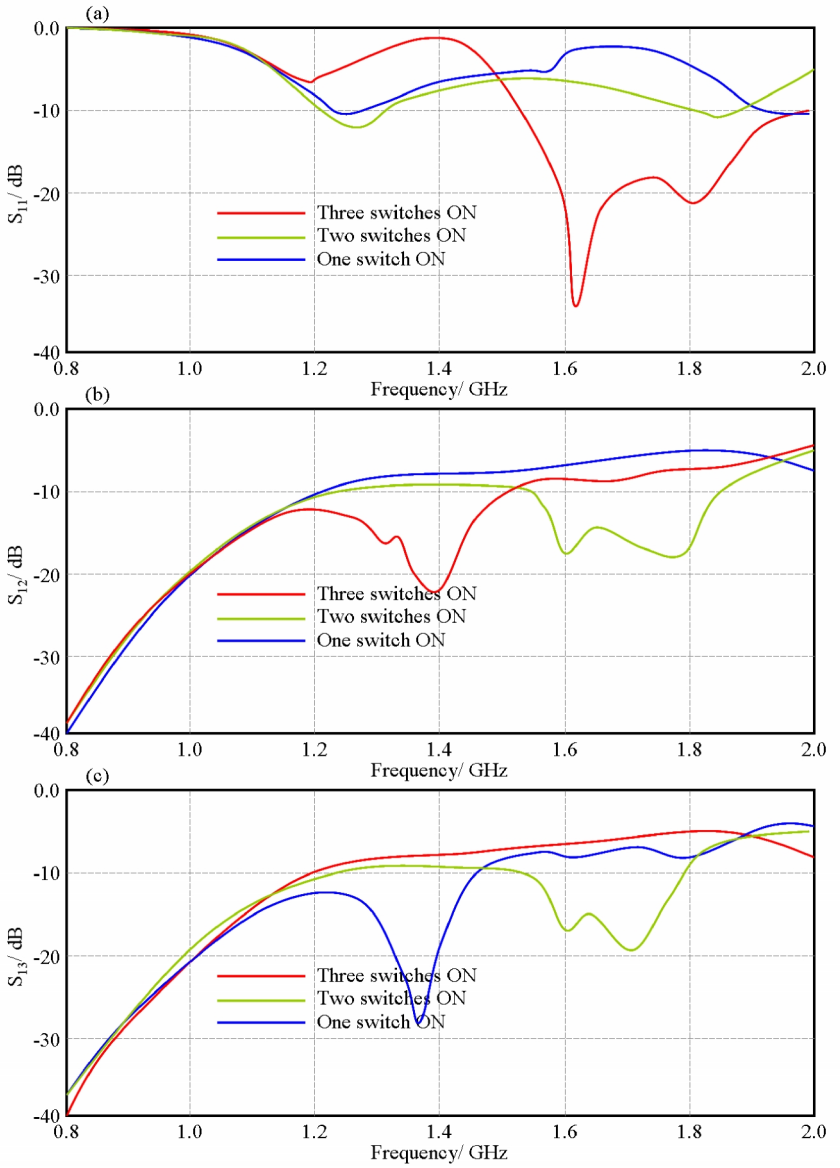

Fig. 4. S-parameters spectra: (a) S_{11}, (b) S_{12}, and (c) S_{13}.

For a MIMO system, the two adjacent antenna elements, the envelope correlation between the antenna elements is given by [6]

$$\rho_e = \frac{\left|S_{ii}^* S_{ij} + S_{ji}^* S_{jj}\right|^2}{[1-(\left|S_{ii}\right|^2 + \left|S_{ji}\right|^2)][1-(\left|S_{jj}\right|^2 + \left|S_{ij}\right|^2)]} \quad (1)$$

where *i* and *j* are for the first and the second antenna elements, respectively. The correlation envelop is evaluated between the first element with the second element and the first element with third element in terms of S_{12} and S_{13}, respectively as seen in Fig. 5.

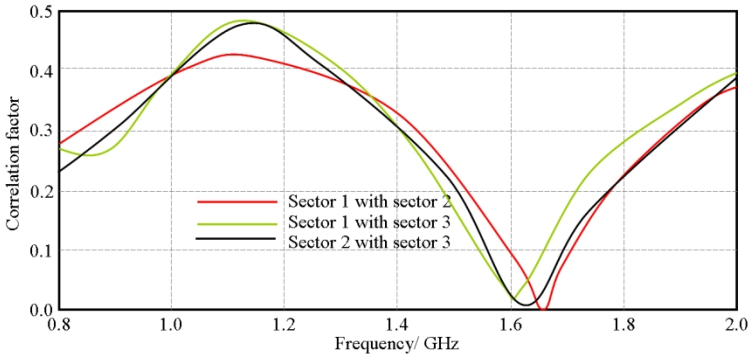

Fig. 5. Correlation profile among 1, 2, and 3 sectors

In Fig. 6, the radiation patterns in the *E*- (Theta=90) and *H*- (Phi=90) planes are displayed at 1.2 GHz and 1.6 GHz when the three switches are ON. The values of the antenna gain, beam width, main lobe direction are listed in Table 2.

Table 2. Antenna array performance

Values				
Performance	1.2 GHz	Sector 1	Main lobe magnitude	1.8 dB
			Main lobe direction	214.0°
			Beam Width	86.5°
		Sector 2	Main lobe magnitude	1.8 dB
			Main lobe direction	336.0°
			Beam Width	86.4°
		Sector 3	Main lobe magnitude	2.0 dB
			Main lobe direction	95.0°
			Beam Width	85.0°
	1.6 GHz	Sector 1	Main lobe magnitude	2.9 dB
			Main lobe direction	214.0°
			Beam Width	87.5°
		Sector 2	Main lobe magnitude	2.9 dB
			Main lobe direction	335.0°
			Beam Width	87.4°
		Sector 3	Main lobe magnitude	2.8 dB
			Main lobe direction	96.0°
			Beam Width	87.8°

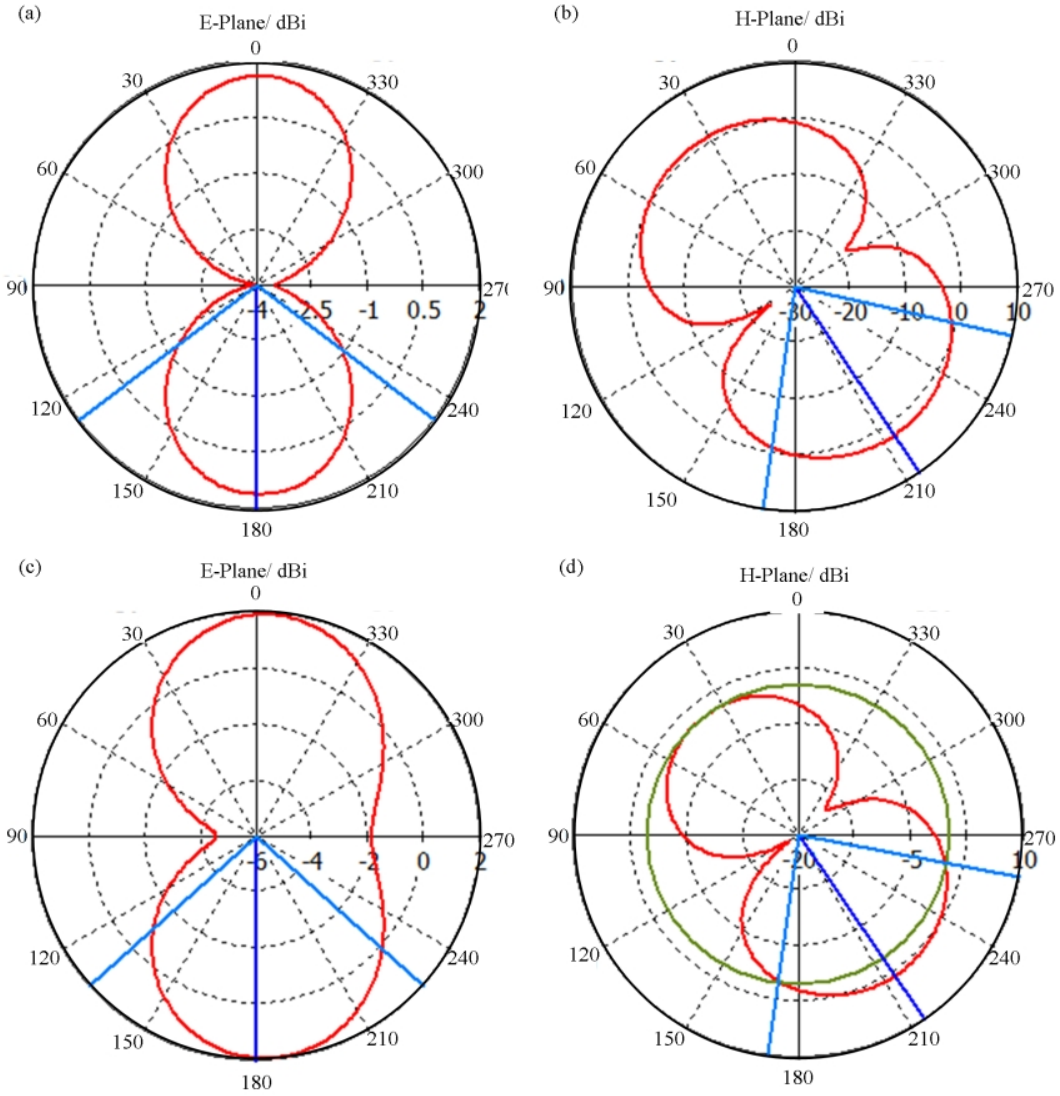

Fig. 6. Far field radiation patterns: (a) E-plane at Theta = 90^O and (b) H-plane at Phi = 90^O for 1.2 GHz. (c) E-plane at Theta = 90^O and (D) H-plane at Phi = 90^O for 1.6 GHz

The validation is attempted using another solver based on FD formulations to study the antenna array performance. An excellent agreement is achieved in terms of S-parameters and radiation patterns as can be seen in Fig. 7.

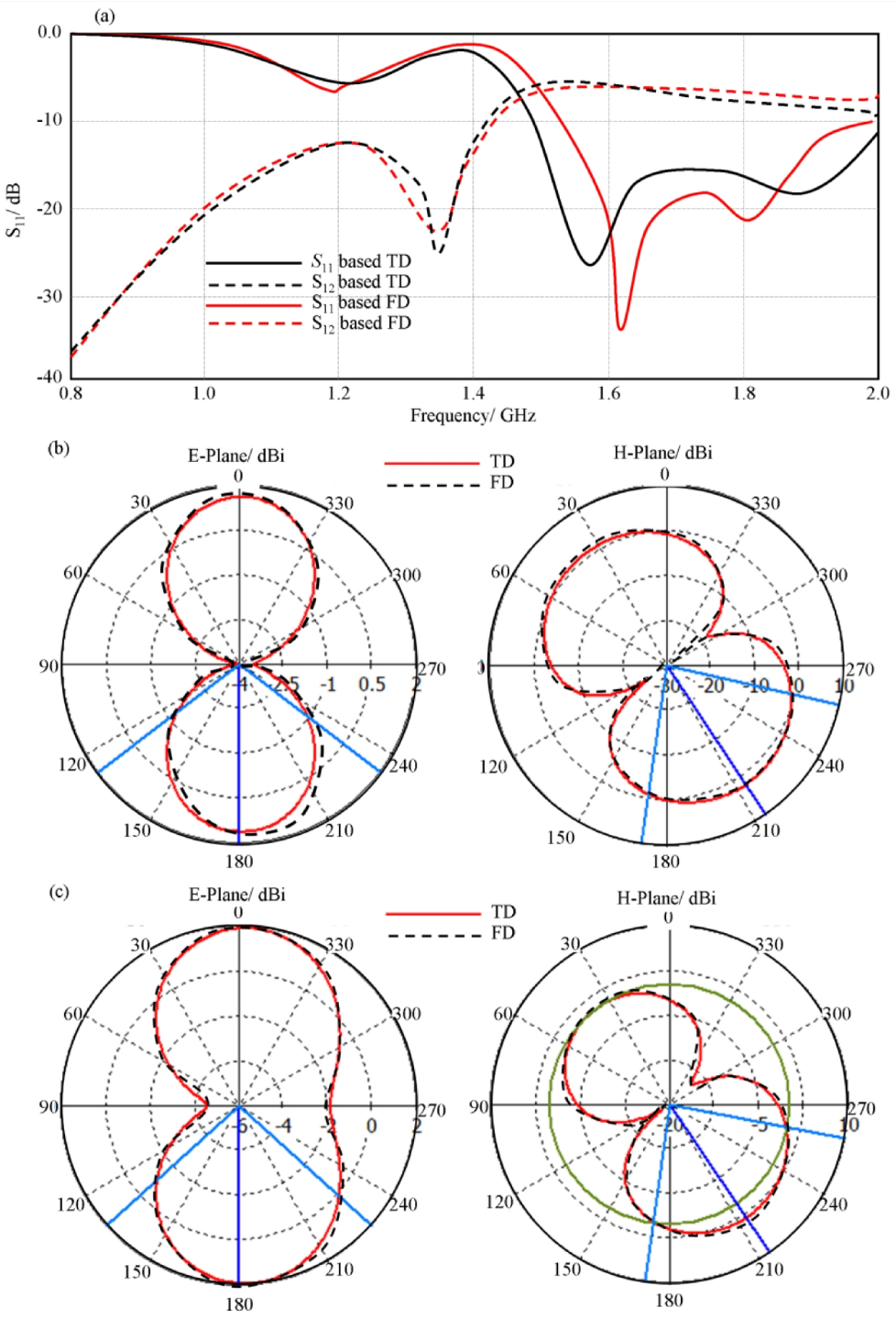

Fig. 7. Antenna performance validation using TD and FD formulations based on CST MWS 3 patches ON: (a) S_{11}, (b) Radiation patterns at 1.2 GHz, (c) Radiation Patterns at 1.6 GHz

4. CONCLUSION

The eliminating of frequency reuse principle in the mobile Ad Hoc system using MIMO antenna array among the sectors of the unit cell is inspected in this paper. To realize this achievement, an antenna array of size of 10×10 cm^2 is considered with using high diversity among antenna sectors. The single antenna sector is constructed from three patches that are connected to feeding transmission network through pin diodes, as switches, that are erected on an FR-4 substrate. Each single element of the antenna differentiated in the space with 120^o rotationally. The antenna performance is characterized from 0.8 GHz to 2 GHz in terms of *S*-parameters and radiation patterns with different switching OFF/ON strategies. It is found that the antenna low correlation factor and end fire radiation at the main lobe direction around 1.2 GHz and 1.5 GHz. A numerical investigation based on FIT is conducted using CST MWS to evaluate the antenna performance. Finally, two different numerical solutions based on TD and FD solvers for CST MWS formulations are conducted to perform a validation for the achieved results.

ACKNOWLEDGEMENTS

The authors would like to thank the Engineering Collage/ Department of Electrical Engineering at UPM for their valuable support during the numerical simulations.

COMPETING INTERESTS

Authors declare that there are no competing interests.

REFERENCES

1. Foschini GJ, Gans MJ. On limits of wireless communications in a fading environment when using multiple antennas," Wireless Personal Communications. 1998;6(3):311–335.
2. Vaughan, Andersen J. Antenna diversity in mobile communications," IEEE Transactions on Vehicular Technology. 1987;36(4):149–172.
3. Quan XL, Li R-L, Wang JY, Cui YH. Development of a broadband horizontally polarized omnidirectional planar antenna and its array for base stations," Progress In Electromagnetics Research. 2012;128:441-456.
4. Wei K, Zhang Z, Feng Z. Design of a dualband omnidirectional planar microstrip antenna array. Progress In Electromagnetics Research. 2012;126:101-120.
5. Costa F, Genovesi S, Monorchio A. A frequency selective absorbing ground plane for low-RCS microstrip antenna arrays. Progress in Electromagnetics Research. 2012;126:317-332.
6. Elwi TA, Al-Rizzo HM, Bouaynaya N, Hammood MM, Al-Naiemy Y. Theory of gain enhancement of UC-PBG antenna structures without invoking Maxwell's equations: An array signal processing approach. Progress in Electromagnetics Research. 2011;34:15-30.
7. Wang M, Wu W, Fang D. Uniplanar single corner-FED dual-band dual-polarization patch antenna array. Progress in Electromagnetics Research Letters. 2012;30:41-48.
8. Abedin MF, M Ali. Effects of a smaller unit cell planar EBG structure on the mutual coupling of a printed dipole array. IEEE Antennas and Wireless Propagation Letters. 2005;4:274-276.

9. Xie H-H, Jiao Y-C, Chen L-N, Zhang F-S. An effective analysis method for EBG reducing patch antenna coupling," Progress in Electromagnetics Research Letters. 2011;21:187-193.
10. Capet N, Martel C, Sokoloff J, Pascal O. Optimum high impedance surface configuration for mutual coupling reduction in small antenna arrays," Progress In Electromagnetics Research B. 2011;32:283-297.
11. Yang F, Rahmat-Samii Y. Microstrip antennas integrated with electromagnetic band gap (EBG) structures: A low mutual coupling design for array applications," IEEE Transactions on Antennas and Propagation. 2003;(51)10:2936-2946.
12. Andersen J, Rasmussen H. Decoupling and descattering networks for antennas," IEEE Trans. Antennas Propag. 1976;24(6):841–846.
13. Chen S-C, Wang Y-S, Chung S-J. A decoupling technique for increasing the port isolation between two strongly coupled antennas. IEEE Trans. Antennas Propag. 2008;56(12):3650–3658.
14. Sievenpiper D, Zhang L, Broas R, Alexopolous N, Yablonovitch E. High-impedance electromagnetic surfaces with a forbidden frequency band. IEEE Trans. Microw. Theory Tech. 1999;47(11):2059–2074.
15. Bait-Suwailam MM, Boybay MS, Ramahi OM. Mutual coupling reduction in MIMO antennas using artificial magnetic materials," in the 13th International Symp. on Antenna Technology and Applied Electromagnetics (ANTEM/URSI). 2009;1–4.
16. Lee JH, Cheng CC. Spatial correlation of multiple antenna arrays in wireless communication systems. Progress in Electromagnetics Research. 2012;132:347-368.
17. Lee JH, Chen YL. Performance analysis of antenna array beamformers with mutual coupling effects. Progress in Electromagnetics Research B. 2011;33:291-315.
18. Rahmat-Samii Y, Yang F. Electromagnetic Band Gap Structure in Antenna Engineering. Cambridge University Press, Cambridge, UK; 2009.
19. Wang T, Yin YZ, Yang J, Zhang YL, Xie JJ. Compact triple-band antenna using defected ground structure for WLAN/WiMAX applications. Progress in Electromagnetics Research Letters. 2012;35:155-164.
20. Iluz Z, Shavit R, Bauer R. Microstrip antenna phased array with electromagnetic bandgap substrate. IEEE Transactions on Antennas and Propagation. 2004;52(6):1446-1453.
21. Rajo-Iglesias E, Quevedo-Teruel O, Inclan-Sanchez L. Mutual coupling reduction in patch antenna arrays by using a planar EBG structure and multilayer dielectric substrate. IEEE Transactions on Antennas and Propagation. 2008;56(6):1648-1655.
22. Chen Z, Ban YL, Chen JH, Li JLW, Wu YJ. Bandwidth enhancement of LTE/WWAN printed mobile phone antenna using slotted ground structure. Progress in Electromagnetics Research. 2012;129:469-483.
23. Wang X, Zhang M, Wang SJ. Practicability analysis and application of PBG structures on cylindrical conformal microstrip antenna and array. Progress in Electromagnetics Research. 2011;115:495-507.
24. Yuan CP, Chang TH. Modal analysis of metal-stub photonic band gap structures in a parallel-plate waveguide. Progress in Electromagnetics Research. 2011;119:345-361.
25. Ederra I, Iriarte JC, Gonzalo R, de Maagt P. Surface waves of finite size electromagnetic band gap woodpile structures. Progress in Electromagnetics Research B. 2011;28:19-34.
26. Li Y, Fan M, Chen F, She J, Z Feng. A novel compact electromagnetic-bandgap (EBG) structure and its applications for microwave circuits. IEEE Transactions on Microwave Theory and Techniques. 2005;53:183-190.

27. Xu F, Wang ZX, Chen X, Wang XA. Dual band-notched UWB antenna based on spiral electromagnetic-bandgap structure. Progress in Electromagnetics Research B. 2012;39:393-409.
28. Alam MS, Islam MT, Misran N. Performance investigation of a uni-planar compact electromagnetic bandgap (UC-EBG) structure for wide bandgap characteristics. Proceedings of the 2012 Asia-Pacific Symposium on Electromagnetic Compatibility (APEMC). 2012;637-640. Singapore.
29. Yu A, Zhang X. A novel method to improve the performance of microstrip antenna arrays using a dumbbell EBG structure. IEEE Antennas and Wireless Propagation Letters. 2003;2:170-172.
30. Fei H, Guo H, Liu X, Wang Y. A novel compact EBG structure for mutual coupling reduction in a patch array. PIERS Proceedings, pp. 615-618, Suzhou, China, Sep. 2011;12-16.
31. Assimonis SD, Yioultsis TV, Antonopoulos CS. Computational investigation and design of planar EBG structures for coupling reduction in antenna applications. IEEE Transactions on Magnetics. 2012;48(2):771-774.
32. Elsheakh DN, Iskander MF, Abdallah EA, Elsadek HA, Elhenawy H. Microstrip array antenna with new 2D-electromagnetic band gap structure shapes to reduce harmonics and mutual coupling," Progress In Electromagnetics Research C. 2010;12:203-213.
33. CST Microwave Studio; 2013. 10th Version. Available at: http://www.cst.com.

Peer-review history:
The peer review history for this paper can be accessed here:
http://www.sciencedomain.org/review-history.php?iid=502&id=5&aid=4404